# A Unified Optimization Framework and New Set of Performance Metrics for Robot Leg Design

Chathura Semasinghe[1], Drake Taylor[1], and Siavash Rezazadeh[1]

***Abstract*— This work presents a framework for the simultaneous optimization of motors, transmissions, and mechanisms of different joints of robotic legs with the goal of achieving an energy efficient, precisely controllable and stable locomotion in dynamic environments. This unified framework allowed us to introduce and formulate new performance metrics for the separate evaluation of the system's stabilizing ability during stance and swing. Moreover, through a case study, this design optimization framework was applied to an anthropomorphic robot leg model and the optimal actuation configurations for the leg were obtained. This case study also helped us investigate the relationships among our three objectives (energy efficiency, and stance and swing control). It was shown that while in some cases a clear trade-off exists, it is not always valid and as such, careful consideration of all three objectives is necessary.**

## I. Introduction

Robot leg design has been focused over several decades towards achieving efficient, agile, and stable locomotion with adaptation to different environments. The various objectives that must be considered in the design of robotic legs usually lead to a trade-off between agility, stability, and efficiency. In case of bipedal robots, as a result of their fewer number of legs in comparison with quadrupeds and hexapods, the problem becomes even more challenging, both in terms of design and control. Bipedal robots such as Atlas [1] and ASIMO [2] have shown remarkable locomotion capabilities in the real world situations. However, their costs of transport (as a widely accepted measure of efficiency) are orders of magnitude higher than their biological counterparts [3]. On the other end of the spectrum, robots such as Ranger [4] and Denise [5] with design ideas originated from the passive walkers of McGeer [6], have demonstrated highly efficient locomotion, but at the cost of sacrificing robustness and multi-task abilities. ATRIAS [7] and its descendant, Cassie [8] were attempts to compromise between the use of passive dynamics and multi-task ability. These robots were specifically designed to encapsulate the essential features of spring-loaded inverted pendulum (SLIP) model [9] such as light legs and special leg mechanisms morphology. As a result, although the robots could directly take advantage of features of SLIP for efficiency and control [10], [11], the leg mechanisms and morphologies were very different from those of human legs. Therefore, even though human locomotion can be well characterized by SLIP model [12], the higher-level features of human locomotion (coordination between joints, use of non-negligible leg inertia for onset of the swing, etc.) cannot be encapsulated by these robots and as such, they cannot be much helpful in study of human-like locomotion.

In the present work, we change the framework presented for leg design in [3] to the case of anthropomorphic legs and significantly improve it for the incorporation of a more comprehensive set of performance metrics. However, since we limit ourselves to anthropomorphic legs in this work, we are able to formulate our optimization problem by simultaneous consideration of all design parameters for the actuators and transmission mechanisms. Such an approach has been previously investigated by Mombaur [13] for the energy optimization (i.e., single-objective) of a humanoid robot's link lengths and mass properties. We take a more design-oriented approach by also optimizing other attributes such as actuator mechanisms and their mechanical parts, while considering the effect of the change of the pertaining optimization parameters on the mass properties of the leg segments.

In addition to this unified framework, we explore the (unavoidable) trade-off between efficiency and control in robotic legs. Total cost of transport (TCOT) provides a widely-used metric for measuring the efficiency of legged robots, and it has almost exclusively been the sole optimization objective in the leg optimization works cited above. In contrast, there is no such widely-accepted metric for control and/or agility of legged robots. Acceleration ability [14] and bandwidth [15] have been previously proposed as metrics for the agility of robotic systems. Although both these metrics have direct relationships with the quick response of an actuator, 1) the interaction of different actuators in a multi-joint system is not considered; 2) their relationship with parameters directly affecting the stability of locomotion and fall prevention is unclear; and 3) they are usually defined based on the (single-point) peak/stall torque of the motor which neglects the fact that in legged robots, the fall prevention is strongly related to the performance within a duration of time. Therefore, in the present work, in addition to TCOT (or equivalently, total energy for a given gait cycle) we introduce two new metrics to represent stance and swing phase control quality.

## II. Robotic Leg System Modeling

Since sagittal-plane is by far the dominant plane of motion for different locomotion tasks and maneuvers, similar to [13] and [3], at the present stage of this work, we limit our analysis to sagittal-plane motions and degrees of freedom. The considered robotic leg structure (as shown in Fig. 1(a))

*This work was supported by NSF grant no. 1953908.

[1]The authors are with the Department of Mechanical and Materials Engineering, University of Denver, Denver, CO, 80210, USA {chathura.semasinghe, drake.taylor, siavash.rezazadeh}@du.edu

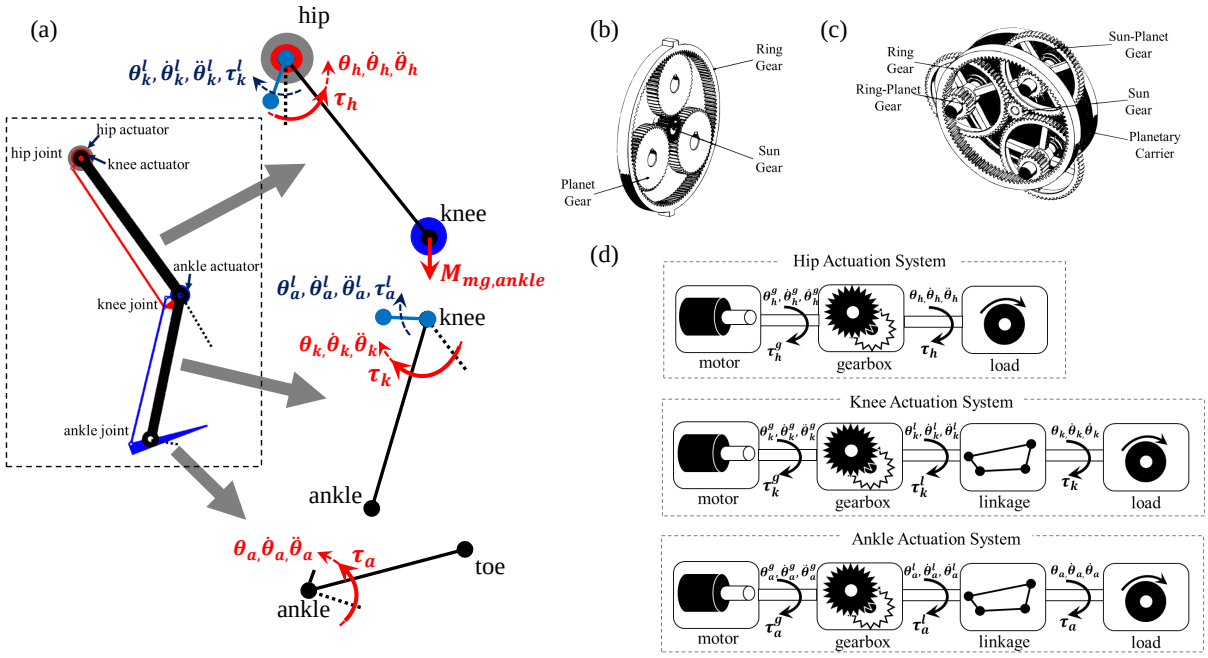


Fig. 1. Robotic leg system: (a) Schematics of the robot leg model. Joint angle and moment trajectories are shown in red. The input links of both knee and ankle linkages, and their angle and moment trajectories are shown in blue. (b) Schematics of a standard planetary gearbox. (c) Schematics of the extended planetary variation. (d) Actuation system configuration for each joint (the icons are for depiction purpose only).

is an anthropomorphic articulated leg mechanism which has three revolute joints for flexion/extension motions of the hip, knee, and ankle joints. The hip joint is actuated through a geared motor placed directly at the hip joint. In contrast, to reduce the distal mass and decrease the inertial forces during acceleration and deceleration of the leg, the knee and ankle motors are placed at the highest points of their respective links and are connected to the joints using a four-bar linkage mechanism. This is a similar approach to what has been taken in numerous leg designs, including MIT Cheetah [16], ATRIAS [7], and Cassie [8] to achieve the same objective.

Although high-bandwidth hydraulic actuators have led to amazing performances in robots such as Atlas [1] and HyQ [17], since one of our main objectives is energy efficiency, we choose electrical actuators over the hydraulic ones. Among this group, brushless DC motors are preferred due to advantages such as durability, less noise, and greater efficiency.

For transmission, planetary gearboxes were chosen, primarily because of their much greater efficiency compared to harmonic gearing [18] and their simpler manufacturing compared to cycloid drives [19]. To avoid extra losses and inertias, we did not consider multi-stage planetary gears and limited our options to the two variations shown in Fig. 1. The first variation, as seen in Fig. 1(b), is a standard planetary gearbox with a set of planets, a sun gear, and a ring gear. This standard version is usually limited to a gear ratio of 10:1. The second variation considered is an extended single-stage planetary gearbox, as seen in Fig. 1(c). The extended single stage option allows for greater gear ratios without affecting efficiency and sound level and by minimal addition of the weight and the geometric space taken [20], [21].

The knee and ankle four-bar linkages (as shown in Fig. 1(a)) are connected to the planetary carrier gearbox outputs in the proximal side, and to the actuated leg link in the distal side using revolute joints. The actuated link for the knee actuator is the shank, and for the ankle actuator is the foot.

## III. System Performance Metrics

Perhaps the most widely-used performance metric for legged robots is their efficiency. Electrical power loss (Joule heating) is usually the most significant source of energy dissipation in electrically-actuated leg mechanisms, and thus, often the optimization of the efficiency is taken equivalent to this loss. Joule heating is proportional to the square of the motor torque [15] and thus, it seems an energy-efficient system can be achieved by using high-speed motors together with high-ratio transmissions (which minimize the motor torque). However, as shown in [16], this is theoretically not true and neglecting their masses, high-torque motors and low transmission ratios can lead to greater efficiencies. Furthermore, high transmission ratios result in high-impedance and non-backdrivable actuation systems, which can make the force and/or impedance control of such systems difficult. Therefore, in recent years, in robots such as MIT Cheetah [16] and Cassie [8], there has been a trend of using high-torque and backdrivable actuators. This helps in achieving lower mechanical actuator impedance and negligible unmodeled dynamics, which in turn reduces the *passive impedance torques* resulted from these effects, and improves the force control quality and impact mitigation during stance phase [20], [22]. A main drawback which has been neglected in these works is the increased mass of the actuator with

the high-torque motors. Because this factor can affect both efficiency and control quality and as one of the contributions of the present work, we formulate and include it in our analysis in this section.

One of the intrinsic complexities of legged locomotion is the distinct roles that the actuators take during stance and swing phases. In the stance phase, the force or impedance control is the dominant paradigm that can mitigate impacts, overcome small disturbances, and help the full-body control, while in the swing phase, position control and foot placement are the primary goals [11]. In accordance with this, for large disturbances, the ability of taking a quick step is crucial for maintaining the balance and preventing falls. As Wisse et al. have pointed out, the robot never falls if the swing leg is put in front of the stance leg fast enough [23]. On the other hand, note that in the case of brushless DC motors (and most other actuator types), the maximum achievable torque decreases with speed. This further complicates the stepping speed evaluation, because a metric such as acceleration ability which is based on the motor's peak torque [14], cannot catch the complete stepping process, as it depends on the dynamic characteristics of the motor over a duration of time and not merely its peak torque as a single point.

Therefore, the leg performance metrics can be considered equivalent to three main objectives; 1) minimize the system energy consumption, 2) minimize the passive impedance torque, and 3) minimize the stepping time. The selection of motors and transmissions will have a direct impact on achieving this objectives.

### A. Joint Trajectories

In the present work, we limit our study to an anthropomorphic robot leg model (as discussed in Section II) which follows the normative human joint angle and joint moment trajectories. Also, as noted, we assume that motors and gearboxes add extra masses and inertias to the system, which will demand additional torques to match the joint trajectories from human data. Therefore, the total joint torque, which is termed as *load torque* in this work, will be the combination of human joint moments and other inertial torques due to the masses of motors and gearboxes. This leads to a more realistic optimization of the leg by penalizing the size of the actuators. In this way, the total load torque trajectories, $\tau_{L,j}$ (with $j \in \{h, k, a\}$ for hip, knee, and ankle, respectively) are computed as:

$$\begin{aligned} \tau_{L,h} &= \tau_h + \tau_{m,k} + \tau_{m,a} + \tau_{mg,a} + \tau_{i\alpha,a} + \tau_{g,h} \\ \tau_{L,k} &= \tau_{l,k} + \tau_{m,a} + \tau_{g,k} \\ \tau_{L,a} &= \tau_{l,a} + \tau_{g,a} \end{aligned} \tag{1}$$

where $\tau_h$ is the hip joint moment from human gait data, $\tau_{m,j}$ is the inertial torque due to the rotor inertia of the corresponding motor, $\tau_{mg,a}$ is the gravitational moment due to adding ankle actuator, $\tau_{i\alpha,a}$ is the inertial torque due to mass of the ankle motor and its gearbox, $\tau_{g,j}$ is the inertial torque of the gearwheels of the gearbox at each joint, and $\tau_{l,j}$ is the input moment to the four-bar linkage (using human gait data and the inverse kinematics of the linkage) at each joint. Note that since there is no linkage for the hip joint, we have $\tau_{l,h} = \tau_h$.

### B. Energy Consumption

The first metric to measure the performance of actuation system is the total energy consumption. Since walking and running are the most common locomotion patterns observed in humans [24], we formulated the energy consumption as the weighted sum of the total energy drawn by the motors to follow normative walking and running gait cycles.

Our approach for calculating the energy consumption is an extension of [15]. Here, we also consider the joint load torques generated from the mutual effects of different degrees of freedom in a multi-joint mechanism, as well as different locomotion patterns.

The total motor power $P^i_{t,j}$ for the joint $j$ ($j \in \{h, k, a\}$) and the locomotion pattern $i$ ($i \in \{w, r\}$ for walking and running, respectively) can be obtained from $P^i_{t,j} = P^i_{s,j} + P^i_{m,j} + P^i_{e,j}$, where $P^i_{s,j}$ is the load power, $P^i_{m,j}$ is the power for driving the actuator inertia, and $P^i_{e,j}$ is the Joule heating. Based on [15], the final expression for $P^i_{t,j}$ is obtained as:

$$\begin{aligned} P^i_{t,j} &= \tau_{L,j}\dot{\theta}^i_j + I_{m,j}\ddot{\theta}_m\dot{\theta}_m + b_{m,j}(\dot{\theta}_m)^2 \\ &\quad + \frac{1}{k^2_{m,j}}(I_{m,j}\ddot{\theta}_m + b_{m,j}\dot{\theta}_m + \frac{\tau^i_{L,j}}{\beta_j})^2, \end{aligned} \tag{2}$$

where $I_{m,j}$ is the motor inertia, $b_{m,j}$ is the motor damping, $k_{m,j}$ is the motor constant, and $\beta_j$ is the momentary transmission ratio (gearbox and linkage). By substituting $\dot{\theta}_m = \beta_j\dot{\theta}^i_j$ and $\ddot{\theta}_m = \beta_j\ddot{\theta}^i_j + \dot{\beta}_j\dot{\theta}^i_j$, and integrating, the energy drawn from the electrical source for a given cycle time, $T$ can be calculated as $E^i_{t,j} = \int_0^T P^i_{t,j}\, dt$ . By considering $x$ percent of the walking gait energy and the rest from the running gait energy, the total energy consumption can be formulated as:

$$Q_e = \sum_j^{h,k,a} \Big[\frac{x}{100}E^w_{t,j} + (1 - \frac{x}{100})E^r_{t,j}\Big] \tag{3}$$

This is our first performance metric.

### C. Passive Impedance Torque

During stance phase, the dominant factor for stability of the robot is its ability of accurate force control for whole-body control of the robot and regulation of its interaction with the ground (in the form of ground reaction force). A systems with low mechanical impedance will support good force control due to the minimization of unmodeled dynamics [20]. These unmodeled dynamics exist due to the motor inertia, motor damping, and additional inertias on the load side, and affect the dynamics in the form of additional torque. Because these parameters are in fact the components of the passive impedance of the actuator, as noted before, in this work, we refer to the sum of these additional torques as the passive impedance torque. Passive impedance torques get much greater magnitudes during running compared to walking, and as such, in our analysis for this performance metric, we only consider the stance phase of the running gait.

The passive impedance torque of joint $j$ due to the rotor inertia and damping of the motor can be written as $\tau^d_{m,j} = (I_{m,j}\ddot{\theta}_m + b_{m,j}\dot{\theta}_m)\beta_j$. By substituting $\dot{\theta}_m = \beta_j\dot{\theta}^r_j$ and $\ddot{\theta}_m = \beta_j\ddot{\theta}^r_j + \dot{\beta}_j\dot{\theta}^r_j$, we obtain:

$$\tau^d_{m,j} = (I_{m,j}\ddot{\theta}^r_j + b_{m,j}\dot{\theta}^r_j)(\beta_j)^2 + I_{m,j}\beta_j\dot{\beta}_j\dot{\theta}^r_j \qquad (4)$$

Note that there is an additional inertial torque affecting the hip joint due to the rotational motion of the mass of the ankle actuator ($\tau_{i\alpha,a}$). In addition, the moments of inertia of the gear wheels inside the hip gearbox further increase the torque demanded from the hip motor ($\tau_{g,h}$). Based on this, the average passive impedance torque at the hip joint for the stance phase of the normative running gait can be obtained for the time duration $T^r_s$ :

$$\tau^d_{t,h} = \int_0^{T^r_s} |\tau^d_{m,h} + \tau_{i\alpha,a} + \tau_{g,h}|\, dt, \qquad (5)$$

Note that the integral serves as an average of the passive impedance torque during the cycle and the absolute value ensures that positive and negative passive impedance torques will not cancel each other. Likewise, the passive impedance torques at the knee and ankle joints are generated from the inertia and damping of their respective motors, and the inertial torques in their gearboxes. Therefore, the average passive impedance torque at the knee and ankle joints during the stance phase of the running gait can be obtained from:

$$\tau^d_{t,j} = \int_0^{T^r_s} |\tau^d_{m,j} + \tau_{g,j}|\, dt, \quad j = k, a \qquad (6)$$

Based on this, we define our second performance metric $Q_d$ as the largest of average passive impedance torques for the three joints of the robots:

$$Q_d = \max_j\{\tau^d_{t,j}\}, \quad j = h, k, a \qquad (7)$$

where $\tau^d_{t,j}$s are obtained from (5) and (6).

### D. Stepping Time

As shown in [23], the ability of fast stepping can be considered equivalent to the ability of the robot to prevent itself from falling (defined as global stability in [23]). As such, we design our third performance metric as the shortest time duration that the actuator can follow a predefined swing path, in order to measure the system's fall prevention capability by its quick stepping.

Since the ankle movement during swing phase is relatively negligible compared to the hip and the knee motions, the ankle joint angle is set as fixed at zero during stepping. For the hip and knee motions, two trajectories obtained using fifth-order splines to ensure $C^2$ continuity, and are used to define the joint angles of a typical relatively large step (see Fig. 2). The trajectories have been designed to represent a typical response of disturbance (push) rejection by humans: the hip flexes from vertical to $60^o$ and the knee flexes to $30^o$ and then extends back to its rest position to set the foot on the ground. Each joint's movement is scaled in time to identify the fastest possible swing that the actuation system configuration is capable of performing.

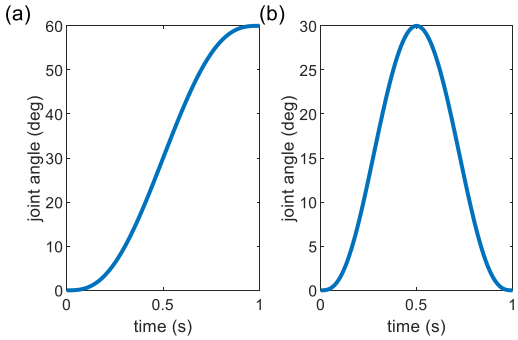


Fig. 2. Considered trajectories for (a) hip, and (b) knee

To calculate the quickest time taken for completing each trajectory by the respective joint, dynamic equations are constructed by modeling the Lagrangian dynamics of the mechanical system. For the analysis of the system dynamics, we use the robot leg model described in Section II. From the Euler-Lagrange equations of the system (with Lagrangian $L$), the reflected torque at each joint can be obtained as:

$$\tau_j = \frac{d}{dt}\left(\frac{\partial L(\theta,\dot{\theta})}{\partial\dot{\theta}_j}\right) - \frac{\partial L(\theta,\dot{\theta})}{\partial\theta_j}, \quad j = h, k \qquad (8)$$

As discussed in the formulation of other performance metrics, in addition to the reflected torque at each joint $j$, there are passive impedance torques generated by the motor inertia and damping, the inertias of the gearwheels, and additional masses. The transmission losses are included using a constant efficiency term $\eta$. Considering these factors, the required motor torque from each motor for following the above predefined trajectories are obtained from:

$$\tau_{mt,j} = \frac{(\tau_j + \tau^d_{m,j} + \tau_{g,j})}{\beta_j\eta^{\text{sgn}(P_{s,j}+P_{m,j})}}, \quad j = h, k \qquad (9)$$

The sign function ensures the consideration of the correct direction of the power flow in the gearbox when we include its efficiency. Note that the stepping time is limited by the maximum motor torque required for following the trajectories. This constraint will be presented in Section IV, along with other constraints of the system.

Finally, as the stepping time $t_{\text{step}}$ is the parameter to be minimized here, we define our third performance metric directly as:

$$Q_t = t_{\text{step}} \quad \text{(subject to the constraints)} \qquad (10)$$

## IV. Optimization

The metrics proposed in Section III assess the performance of the robot leg by energy efficiency, force controlability, and step time for a given actuator configuration. As presented in Section II, the actuation system is comprised of three main components: electric motor, gearbox and four-bar linkage mechanism. The optimization variables include both discrete (motor, gearbox type) and continuous (gearwheels

and linkage parameters). The gearwheel design parameters include number of teeth, modules, and face-width. Based on this, a standard planetary gearbox will have four independent design variables, namely: planet gear teeth number, ring gear teeth number, gear module, and face-width. For the extended planetary gearbox, two additional independent design variables are added: ring-planet gear teeth number and a different gear module for the ring and the ring-planet gears. Also, each four-bar linkage mechanism has three independent design variables for the lengths of the input link, the coupler link, and the output link.

This design problem translates to a standard form of multi-objective optimization as:

$$\begin{bmatrix} (M_h^*, M_k^*, M_a^*) \\ (\{G\}_h^*, \{G\}_k^*, \{G\}_a^*) \\ (\{L\}_k^*, \{L\}_a^*) \end{bmatrix} = \arg\min \left\{ \begin{bmatrix} Q_e \\ Q_d \\ Q_t \end{bmatrix} \right\} \tag{11}$$

where $M_h^*, M_k^*, M_a^*$ are the optimal motor selection for the hip, knee, and ankle joints; $\{G\}_h^*, \{G\}_k^*, \{G\}_a^*$ are the optimal set of design variables for the hip, knee, and ankle gearboxes; and $\{L\}_k^*, \{L\}_a^*$ are the optimal set of design variables for the knee and ankle linkage mechanisms.

The primary constraints related to the optimization problem (11) arise from the linear speed-torque characteristics of the motors. As discussed in [3], this constraint is especially important for untethered systems such as legged robots, where the limited battery voltage makes this constraint dominant over other constraints such as the demagnetization torque. To satisfy this constraint, at all operation instants, we must have:

$$\textbf{C1: } |\tau_m| \leq -k_m^2 |\dot{\theta}_m| + \frac{k_m^2}{k_t} V \tag{12}$$

where $\tau_m$ is the instantaneous motor torque, $\dot{\theta}_m$ is the instantaneous motor speed, $k_t$ is the torque constant, and $V$ is the battery voltage. Moreover, the motor torque cannot violate the demagnetization torque or exceed the maximum current that the driver can provide. Therefore:

$$\textbf{C2: } \tau_m < \min\{k_t i_{max}, \tau_{demag}\} \tag{13}$$

Next, we consider the feasibility of the gearbox design. To avoid failures in the gears, the nominal tangential load on the reference pitch circle of the gear, $F_{t,g}$, should be always less than the allowable tangential load $F_{lim,g}$ calculated from the AGMA bending stress equation [25]. Note that all of the internal gears of the planetary gearbox should satisfy this condition in order to consider the gearbox design feasible. Therefore,

$$\textbf{C3: } F_{t,g} \leq F_{lim,g}, \quad g \in \{\text{ring, sun, planets}\} \tag{14}$$

Finally, the range of the non-singular motion of the four-bar linkage $R_{req,j}$ must be greater than the required range of motion of the corresponding joint $R_{lin,j}$. That is:

$$\textbf{C4: } R_{lin,j} \subset R_{req,j} \tag{15}$$

Based on the optimization problem (11) and the constraints C1-C4, in the next section, we present a case study of an anthropomorphic leg design.

## V. Case Study: Actuation System Design for a Robotic Leg

In this section, a quantitative investigation of the proposed performance metrics for the optimal actuation system selection is presented for the robot leg design described in Section II. As mentioned before, in the present work, we optimize the system for normative human trajectories and do not consider the optimization of the trajectories themselves. Human gait data for running at 3.5 m/s and walking at 1 m/s of respectively 11 and 23 healthy young subjects were picked from the publicly available datasets in [26] and [27]. The gait data were normalized and averaged to obtain the normative cycles for each locomotion pattern. Then, the mass-normalized data such as joint moments were denormalized by assuming a mass of 65 kg as the approximated target mass of the robot. The anthropometric parameters of the human lower limb (segment mass, inertia, length, etc.) were calculated according to [28] for use in the dynamic model of the robot. For this case study, three candidate motors with similar masses were chosen from Allied Motion Megaflux Series (MF0095032, MF0127020, and MF0127032) for each joint. In addition, both types of planetary gearboxes were considered for finding the optimal gearbox for each joint. The optimization problem included all of the constraints presented in Section IV.

Fig. 3(a) shows the optimal Pareto front resulted from solving this optimization problem using MATLAB's `gamultiobj` function with controlled elitist genetic algorithm that ran for 16 hours on a PC with Intel Core i7-8700 3.2GHz processor. The optimal Pareto front consists of 587 Pareto points and each point corresponds to 6 discrete and 24 continuous design variables. As an example, the point highlighted in red represents three optimal motors for each joint (identified by candidate motor number 1, 2, or 3) and three gearbox types (1: standard, 2: extended), six gearbox design parameters for each joint (number of teeth in ring, ring planet and sun planet gear, module for ring and ring planet gear, module for sun and sun planet gear and face-width of the gearwheels, respectively) and three linkage design parameters (lengths of input link, coupler link, and output link, respectively) for each of the knee and ankle linkages.

It is observed that the extended planetary gearbox is the optimal gearbox type for the knee. This is due to the greater torques at the knee joint which demands higher gear ratios. In contrast, for the ankle and hip joints for which the joint moments are smaller than the knee, the standard planetary gearboxes were shown to work. In either case, the combination of high-torque motors and low gear-ratio gearboxes (ratios of 9.3 for the hip, 16.7 for the knee, and 8.6 for the ankle at the highlighted point) resulted in small passive impedance torques compared to the joint moments.

The 2-D snapshots of the results in Fig. 3(b) shows that there is always a trade-off between the energy consumption and passive impedance torque metrics. Unlike this clear trade-off, no obvious monotonic trend can be observed in the relationship between the stepping time and the energy

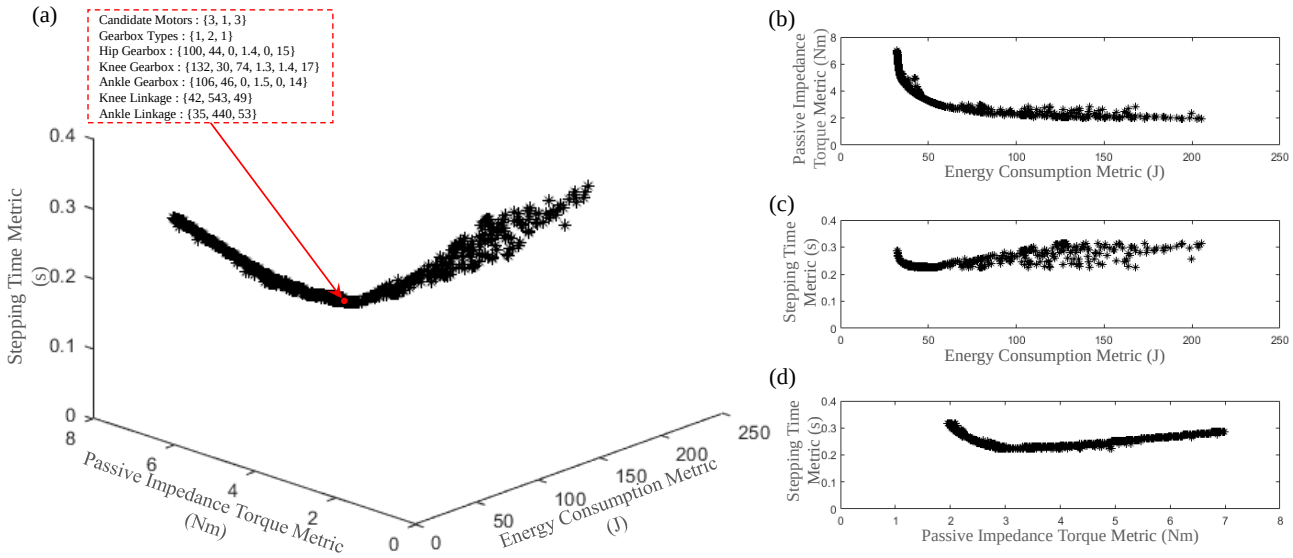


Fig. 3. Case-study results: (a) 3-D Pareto front of the optimal design; and 2-D snapshot of the Pareto front for (b) passive impedance torque versus energy; (c) stepping time versus energy; and (d) stepping time versus passive impedance torque.

metrics (see Fig. 3(c)), and the passive impedance torque and stepping time metrics (Fig. 3(d)). In other words, when the stepping time metric is involved (i.e., Figs. 3(c) and (d)), the trends can be highly case-specific, and failing to consider this metric can result in non-optimal stepping performance and thus, fall prevention ability. This, in turn, proves the importance of considering all three metrics together for the optimal performance of the leg. As any multi-objective problem, the final selection of the optimal actuation system for a legged robot ends with a user-oriented decision, based on the importance of each objective.

## VI. Conclusion

In this paper, we presented an extended framework for the optimal design of the actuation system of a robotic leg by coupling the design of the mechanical parts of the transmission to the electromechanical and dynamical models of the motors and the leg. Furthermore, three performance metrics were proposed to evaluate the actuation system, with the goal of achieving energy efficient, precisely controllable, and globally stable (in the sense of [23]) locomotion. In particular, to measure the controllability and fall prevention capability of the robot, we proposed separate metrics for stance and swing, according to the specific characteristics and control requirements for each of these phases. For the stance phase, due to the great importance of the quality of force and impedance control, the minimization of the passive impedance torque was targeted. In contrast, for the swing, since the fast foot placement is crucial for fall prevention, the stepping time was set as the primary objective. Note that the unified optimization approach for simultaneous optimization of all joints was necessary to formulate these performance metrics. These three objectives, together with 30 design variable and 11 nonlinear constraints (for three motors, three gearboxes and two linkages), formed a multi-objective optimization problem for identifying the optimal actuation mechanisms for the joints of the considered anthropomorphic leg model.

From the case study conducted using the human gait data, it is observed that the Pareto-optimal energy consumption and passive impedance torque metrics of the system have inversely proportional relationship. The cases of Pareto-optimal passive impedance torque versus stepping time, and also energy versus stepping time demonstrate more case-specific relationships and thus emphasize the importance of careful consideration of all three objectives in the design process to achieve the desired performance.

Although this research work considered a relatively general case for the optimal actuation system selection, there are several aspects remaining for future investigations. In particular, further studies on stepping time and its relationship with the other two objectives can reveal more definitive trends and help in more intuitive design guidelines. Moreover, this work can be further extended by solving the co-design problem of simultaneous optimization of joint trajectories and the actuator design parameters. Furthermore, the extension of this work to more general cases such as 3-D leg mechanisms, or to the cases when some of the joints include series elastic actuators are some of other possible directions for future works. Such extensions can serve both for validation of the proposed methods and metrics, and for shedding more light on quantification of the legged robots' performance.

## References

[1] Atlas®. Accessed: Oct. 2020. [Online]. Available: https://www.bostondynamics.com/atlas

[2] M. Hirose and K. Ogawa, "Honda humanoid robots development," *Philos. Trans. Royal Soc. A*, vol. 365, no. 1850, pp. 11–19, 2007.

[3] S. Rezazadeh, A. Abate, R. L. Hatton, and J. W. Hurst, "Robot leg design: A constructive framework," *IEEE Access*, vol. 6, pp. 54 369–54 387, 2018.

[4] P. A. Bhounsule, J. Cortell, A. Grewal, B. Hendriksen, J. G. D. Karssen, C. Paul, and A. Ruina, "Low-bandwidth reflex-based control for lower power walking: 65 km on a single battery charge," *Int J Rob Res*, vol. 33, no. 10, 2014.

[5] M. Wisse, G. Keliksdal, J. Van Frankenhyyzen, and B. Moyer, "Passive-based walking robot," *IEEE Robot Autom Mag*, vol. 14, no. 2, pp. 52–62, 2007.

[6] T. McGeer, "Passive dynamic walking," *Int J Rob Res*, vol. 9, no. 2, pp. 62–82, 1990.

[7] C. Hubicki, J. Grimes, M. Jones, D. Renjewski, A. Spröwitz, A. Abate, and J. Hurst, "ATRIAS: Design and validation of a tether-free 3d-capable spring-mass bipedal robot," *Int J Rob Res*, vol. 35, no. 12, pp. 1497–1521, 2016.

[8] A. Abate, "Mechanical design for robot locomotion," Ph.D. dissertation, Oregon State Univ., Corvallis, OR, 2018.

[9] R. Blickhan, "The spring-mass model for running and hopping," *J Biomech*, vol. 22, no. 11-12, pp. 1217–1227, 1989.

[10] S. Rezazadeh, C. Hubicki, M. Jones, A. Peekema, J. Van Why, A. Abate, and J. Hurst, "Spring-Mass Walking With ATRIAS in 3D: Robust Gait Control Spanning Zero to 4.3 KPH on a Heavily Underactuated Bipedal Robot," in *ASME Dynamic Systems and Control Conference (DSCC)*, Columbus, OH, 2015, p. V001T04A003.

[11] S. Rezazadeh and J. W. Hurst, "Control of ATRIAS in three dimensions: Walking as a forced-oscillation problem," *Int J Rob Res*, vol. 39, no. 7, pp. 774–796, 2020.

[12] H. Geyer, A. Seyfarth, and R. Blickhan, "Compliant leg behaviour explains basic dynamics of walking and running," *Proc. Royal Soc. B*, vol. 273, no. 1603, pp. 2861–2867, 2006.

[13] K. Mombaur, "Using optimization to create self-stable human-like running," *Robotica*, vol. 27, no. 3, pp. 321–330, 2009.

[14] D.-Z. Chen and L.-W. Tsai, "Kinematic and dynamic synthesis of geared robotic mechanisms," *J Mech Des*, vol. 115, no. 2, pp. 241–246, 1993.

[15] S. Rezazadeh and J. W. Hurst, "On the optimal selection of motors and transmissions for electromechanical and robotic systems," in *IROS*, Chicago, IL, 2014, pp. 4605–4611.

[16] S. Seok, A. Wang, M. Y. Michael Chuah, D. J. Hyun, J. Lee, D. M. Otten, J. H. Lang, and S. Kim, "Design Principles for Energy-Efficient Legged Locomotion and Implementation on the MIT Cheetah Robot," *IEEE ASME Trans Mechatron*, vol. 20, no. 3, pp. 1117–1129, 2015.

[17] C. Semini, N. G. Tsagarakis, E. Guglielmino, M. Focchi, F. Cannella, and D. G. Caldwell, "Design of HyQ–a hydraulically and electrically actuated quadruped robot," *Proc. Inst. Mech. Eng. Pt. I: J. Syst. Contr. Eng.*, p. 0959651811402275, 2011.

[18] J. Meyer and A. Petrou, "The relative merits of three different power transmission systems for precision tracking space mechanisms," in *7th European Space Mechanisms and Tribology Symposium*, Noordwijk, the Netherlands, 1997.

[19] J. Liu, B. Chen, S. Matsumura, C. Li, and H. Houjoh, "Design of a novel cycloid drive with a cycloid-arc gear and analysis of its meshing characteristic," *J. Adv. Mech. Des. Syst. Manuf.*, vol. 6, no. 2, pp. 310–322, 2012.

[20] T. Elery, S. Rezazadeh, C. Nesler, and R. D. Gregg, "Design and validation of a powered knee–ankle prosthesis with high-torque, low-impedance actuators," *IEEE Trans Robot*, 2020.

[21] V. Gupta and A. Deb, "Analysis of variable gear system on energy consumption in electric vehicle using simulation tool," *Int J of Sim Syst Sci & Tech*, pp. 7–11, 2012.

[22] P. M. Wensing, A. Wang, S. Seok, D. Otten, J. Lang, and S. Kim, "Proprioceptive actuator design in the mit cheetah: Impact mitigation and high-bandwidth physical interaction for dynamic legged robots," *IEEE Trans Robot*, vol. 33, no. 3, pp. 509–522, 2017.

[23] M. Wisse, A. L. Schwab, R. Q. van der Linde, and F. C. van der Helm, "How to keep from falling forward: Elementary swing leg action for passive dynamic walkers," *IEEE Trans on Robot*, vol. 21, no. 3, pp. 393–401, 2005.

[24] G. Cappellini, Y. P. Ivanenko, R. E. Poppele, and F. Lacquaniti, "Motor patterns in human walking and running," *J. Neurophysiol.*, vol. 95, no. 6, pp. 3426–3437, 2006.

[25] S. R. Schmid, B. J. Hamrock, and B. O. Jacobson, *Fundamentals of machine elements*. CRC Press, 2014.

[26] R. K. Fukuchi, C. A. Fukuchi, and M. Duarte, "A public dataset of running biomechanics and the effects of running speed on lower extremity kinematics and kinetics," *PeerJ*, vol. 5, p. e3298, 2017.

[27] C. A. Fukuchi, R. K. Fukuchi, and M. Duarte, "A public dataset of overground and treadmill walking kinematics and kinetics in healthy individuals," *PeerJ*, vol. 6, p. e4640, 2018.

[28] D. A. Winter, *Biomechanics and motor control of human movement*. John Wiley & Sons, 2009.